INVESTIGATION OF FLUORESCENCE EFFECTS OF $EU(TTA)_3(H_2O)_2$ AND $EU(TTA)_3(PHEN)$ COMPLEXES IN THE PRESENCE OF OTHER LANTHANIDE METAL IONS

Ngoc Doan Vu[1,*], Quang Tuan Do[1], Minh Dong Le[1], Hai Thuong Cao[1]

[1]*Faculty of Physics and Chemical Engineering, Le Quy Don Technical University*

Abstract

In this study, we explore the fluorescence behavior of $Eu(TTA)_3(H_2O)_2$ and $Eu(TTA)_3(Phen)$ complexes in the presence of various other lanthanide metal ions, with the objective of ensuring diversity in the raw material sources for military purposes. The fluorescence properties of these complexes are investigated to understand their potential interactions with other lanthanide ions and their effects on fluorescence emission. Spectroscopic analysis is conducted to examine how the presence of different lanthanide ions influences the fluorescence emission of $Eu(TTA)_3(H_2O)_2$ and $Eu(TTA)_3(Phen)$ complexes. Product structure characteristics are determined by IR, UV-Vis, and EDX spectroscopy. The optical properties of the complex are studied by fluorescence spectroscopy. The results indicate that the structure $Eu_xM_{1-x}(TTA)Phen$ (M: Tb, Nd, Pr; x = 0.1; 0.5; 0.9; 1.0) gives stronger luminescence at ignited wavelengths λ_{ex} = 385 nm.

***Keywords**: Lanthanide; multicomponent reaction; fluorescence.*

1. Introduction

The use of chemical weapons in warfare is a deeply concerning and internationally prohibited act. However, in the past, there have been instances of chemical weapons being used in conflicts and wars [1]. Throughout the Vietnam War (1954-1975), the United States military employed chemical weapons in the battlefields of South Vietnam, including Agent Orange and other chemicals, to destroy forests, weaken food supplies, and disrupt the living environment of entire ecosystems. The consequences of these actions continue to persist to this day. Military chemical toxins are highly dangerous substances capable of causing mass casualties [2], particularly nerve agents like sarin due to their relatively rapid effects at low concentrations [3, 4]. They are difficult to detect, diminishing combat effectiveness and readiness.

The analysis and detection of these chemical agent groups are of utmost importance in military and defense contexts. Therefore, armed forces worldwide continuously research and develop methods for detection, such as: Rapid pesticide testing for two groups: Organophosphate and Carbamate VPR10; AChE enzyme

[*] Corresponding author email: doanvn@lqdtu.edu.vn
DOI: 10.56651/lqdtu.jst.v2.n02.770.pce

detection for nerve agents containing phosphorus compounds; AP-20 Kitagawa-Visitech gas detector pump for rapid detection of toxic gases; Quick detection paper strips such as Calid-3 for rapid identification of chemical agents... One of the emerging methods currently receiving attention from scientists worldwide is fluorescence-based detection [5-7]. Fluorometric analysis refers to a group of optical analysis methods based on the selective interaction between the substance to be identified and the radiation energy in the ultraviolet, visible, or infrared regions. Within a short period of time, chemical toxins can be detected and accurately identified. Based on utilizing the fluorescence properties of Lanthanide complex compounds to identify organophosphorus chemical toxins, a type of toxin of particular interest globally, especially in military applications.

In research on detecting toxins through fluorescence phenomena, enhancing the fluorescence effect of the complex is important for several reasons. In 2007, Rudevich and co-workers reported the first fluorescent probe **1** for sensing of phosgene based on two different coumarin derivatives (one is donor, and the other is acceptor) in which amino group served as the reaction site for phosgene [8]. As a cross-linking agent, phosgene quickly reacted with two amino groups of probe **1** to form a urea linker (Fig. 1).

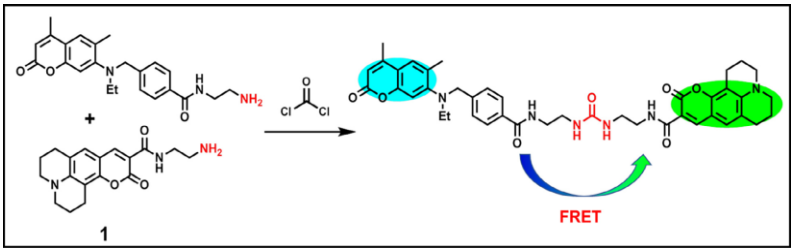

*Fig. 1. The chemical structure and working mechanism of probe **1** for sensing of phosgene.*

Kumar *et al.* utilized a chromogenic and fluorescent probe system **52** for the detection of sulfur mustard simulants [9]. In the absence of SM, dithiol forms colorless adducts with SQ through a nucleophilic substitution reaction SN_2 involving thiol, as depicted in Fig. 2.

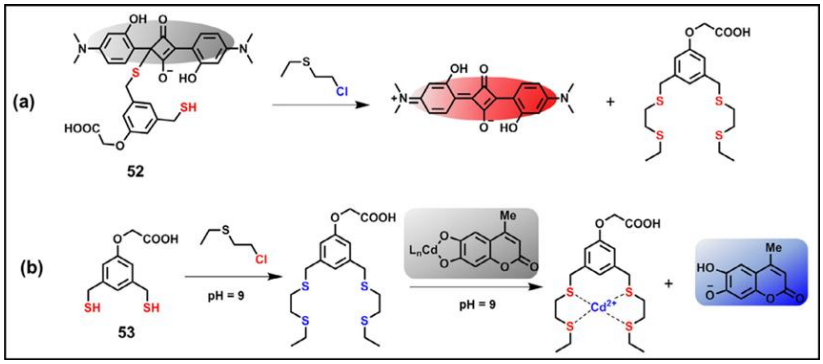

Fig. 2. Fluorescence reaction of thiol/thiophenol probes with SM.

Complexes of Lanthanide ions have been extensively researched for their ability to convert electrical energy into light energy and vice versa. This property holds promise for their application in optoelectronic devices such as solar cells and sensors. Recent studies have indicated that combining them with chromophores as ligands significantly enhances their fluorescence capability. Additionally, it has been demonstrated that these complexes can form complexes with organophosphorus compounds [10-14].

Schwierking and Menzel reported rapid luminescence quenching of a series of thenoyltrifluoroacetone (TTA) and 1,10-phenanthroline (Phen) lanthanide complexes when exposed to either the fluorophosphate simulant diisopropyl fluorophosphate (DFP) or HF vapour [15]. The mechanism for luminescence quenching with DFP was proposed to proceed by an initial hydrolysis of the phosphorus-fluorine bond to liberate a fluoride anion followed by subsequent displacement of the TTA or Phen ligands by means of a competitive binding process (Fig. 3).

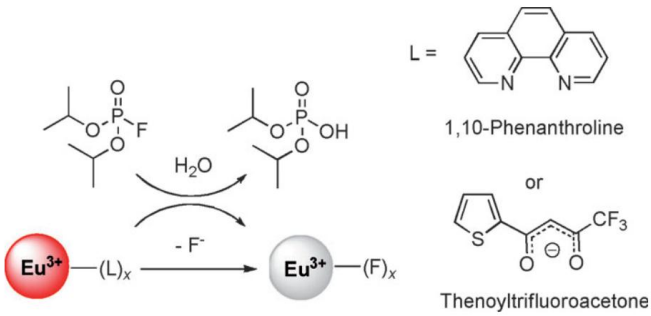

Fig. 3. Proposed mechanism for the luminescence quenching of the europium complex upon exposure to DFP (L=Phen or TTA).

During the synthesis process of the complex, our research aimed to explore the potential of incorporating metals such as Tb, Nd, Pr, alongside Eu, to augment the fluorescence properties of the synthesized complex. This strategic selection of metals enabled us to delve into their respective contributions towards enhancing the fluorescence effect, laying the groundwork for a comprehensive understanding of their synergistic interactions within the complex. Throughout the research project, our primary focus remained steadfast on enhancing the fluorescence capability of the synthesized complex. This emphasis was driven by our overarching goal of developing practical applications, particularly in the realm of nerve agent detection methods. By prioritizing the enhancement of fluorescence capabilities, we aimed to bolster the sensitivity and efficacy of detection methodologies, ultimately contributing to advancements in defense and security technologies. Moreover, our endeavors extended

towards diversifying inputs for military applications, ensuring robustness and integrity in weapons applications. By broadening the spectrum of inputs, we sought to fortify the reliability and versatility of military systems, thereby reinforcing their effectiveness in addressing evolving security challenges. Through these concerted efforts, we aimed to bolster the resilience and efficacy of military technologies, safeguarding national security interests.

2. Experiment

Chemicals for synthesizing Ln complex; $EuCl_3.6H_2O$; $TbCl_3.6H_2O$; $NdCl_3.6H_2O$; $Pr(NO)_3.6H_2O$; HTTA: 2-thenoyl trifluoroacetone; Phen: 1,10-phenanthroline; NaOH; from Sigma, America. Pure chemicals used do not need to be refined again. The solvents used were purchased from China and were distilled before the experiment. The structure of the product is determined based on: IR spectrum measured by IR Spectrum two (PerkinElmer) machine at the Department of Chemical Defense, Military Technical Academy; UV-Vis spectrum was taken at the Department of Environmental Engineering; Fluorescence spectrum method was taken by Fluorolog-3 machine and EDX spectrum was taken by HORIBA model 7593-H machine mounted on FESEM HITACHI S-4800 system at Institute of Chemistry - Vietnam Academy of Science and Technology.

Synthesis of $Eu(TTA)_3(H_2O)_2$ complex

A solution of 1.0 g HTTA (4.5 mmol) in 20.0 mL C_2H_5OH (v/v, 95%), 0.18 g of 1 M NaOH solution (4.5 mmol) was added to a 50.0 mL round-bottomed flask and stirred well. Slowly add a solution containing 0.55 g $EuCl_3.6H_2O$ (1.5 mmol; 1M). The reaction was heated at 60°C for 8 hours. Stop the reaction and bring it to room temperature, the precipitate was filtered using a Buchner funnel, washed with ethanol three times (20.0 mL), dried, and stored in a desiccator.

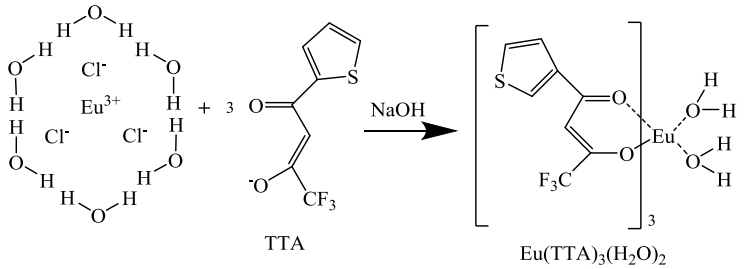

Fig. 4. Reaction equation of $Eu(TTA)_3(H_2O)_2$.

Synthesis of $Eu(TTA)_3(Phen)$ complex

Add a solution containing 0.333 g HTTA (1.5 mmol) and 0.099 g Phen (0.5 mmol) dissolved in 5.0 mL of ethanol to a glass beaker, stir continuously for 2 hours to obtain

solution A. 0.129 g $EuCl_3.6H_2O$ (0.5 mmol) was dissolved in 5.0 mL of ethanol contained in another glass beaker, stirred for 2 hours to obtain solution B. Solution B was slowly added to solution A, stirred continuously for 4 hours, and the pH was adjusted to 8-9 by adding NaOH to obtain the compliiex precipitate. The precipitate was filtered and dried at 40^{o}C in an oven for 4 hours. The product obtained was $Eu(TTA)_3(Phen)$ complex powder.

Synthesis of $Eu_xTb_{1-x}(TTA)_3(Phen)$ complex

Add a solution containing 0.333 g HTTA (1.5 mmol) and 0.099 g Phen (0.5 mmol) dissolved in 5.0 mL of ethanol to a conical flask, stir continuously for 2 hours to obtain solution A. Add a mixture of $EuCl_3.6H_2O$ and $TbCl_3.6H_2O$ (0.5 mmol) in the ratio of x = 0.1; 0.5; 0.9, respectively, dissolved in 5.0 mL of ethanol contained in another conical flask, stirred for 2 hours to obtain solution B. Solution B was slowly added to solution A, stirred continuously for 4 hours, and the pH was adjusted to 8-9 by adding NaOH to obtain the complex precipitate. The precipitate was filtered and dried at 40^{o}C in an oven for 4 hours. The product obtained was $Eu_xTb_{1-x}(TTA)_3(Phen)$ complex powder.

Synthesis of $Eu_xNd_{1-x}(TTA)_3(Phen)$ complex

Add a solution containing 0.333 g HTTA (1.5 mmol) and 0.099 g Phen (0.5 mmol) dissolved in 5.0 mL of ethanol to a conical flask, stir continuously for 2 hours to obtain solution A. Add a mixture of $EuCl_3.6H_2O$ and $NdCl_3.6H_2O$ (0.5 mmol) in the ratio of x = 0.1; 0.5; 0.9, respectively, dissolved in 5.0 mL of ethanol contained in another conical flask, stirred for 2 hours to obtain solution B. Solution B was slowly added to solution A, stirred continuously for 4 hours, and the pH was adjusted to 8-9 by adding NaOH to obtain the complex precipitate. The precipitate was filtered and dried at 40^{o}C in an oven for 4 hours. The product obtained was $Eu_xNd_{1-x}(TTA)_3(Phen)$ complex powder.

Synthesis of $Eu_xPr_{1-x}(TTA)_3(Phen)$ complex

Add a solution containing 0.333 g HTTA (1.5 mmol) and 0.099 g Phen (0.5 mmol) dissolved in 5.0 mL of ethanol to a conical flask, stir continuously for 2 hours to obtain solution A. Add a mixture of $EuCl_3.6H_2O$ and $Pr(NO)_3.6H_2O$ (0.5 mmol) in the ratio of x = 0.1; 0.5; 0.9, respectively, dissolved in 5.0 mL of ethanol contained in another conical flask, stirred for 2 hours to obtain solution B. Solution B was slowly added to solution A, stirred continuously for 4 hours, and the pH was adjusted to 8-9 by adding NaOH to obtain the complex precipitate. The precipitate was filtered and dried at 40^{o}C in an oven for 4 hours. The product obtained was $Eu_xPr_{1-x}(TTA)_3(Phen)$ complex powder.

3. Results and discussion

3.1. Synthesis of Lanthanides complexes

The synthesized complexes were characterized by IR spectroscopy to confirm the presence of functional groups in the complexes. The IR spectra of Phen, HTTA and $Eu(TTA)_3Phen$ are shown in Fig. 5. The bands with peaks at 1587, 853 and 739 cm^{-1} are assigned to the C=N and C–H deformation vibrations of Phen, respectively. This indicates that the chemical bonds are formed between the rare earth ion and the nitrogen atom in the 1,10-Phenanthroline chain. Moreover, the IR spectrum of HTTA shows a weak band at 3118 cm^{-1}, which can be assigned to the mC–H of the thiophene ring. This band is observed at frequencies (c: 3089 cm^{-1}; d: 3089 cm^{-1}) in all the complexes. Furthermore, the typical asymmetric mC=O (HTTA) group vibrations are found at around 1662 and 1643 cm^{-1}, and shifted to 1627 and 1598 cm^{-1} upon complexation, indicating the bond formation between rare earth ions and the oxygen atom in the carbonyl group, thus confirming the formation of the complexes. In addition, the spectrum of $Eu(TTA)_3Phen$ shows no significant absorption bands in the range of 3000–3500 cm^{-1}, suggesting that water is not coordinated to the ninth coordination site of Eu^{3+} and the coordinated ligands protect the metal ion from water in the crystal structure. This result is in good agreement with previously published works [15].

From the IR spectrum analysis results in Fig. 5 of the $Eu(TTA)_3(H_2O)_2$ complex, it is evident that there are characteristic absorption peaks of $\nu_{C=O}$ (1600-1710 cm^{-1}) and $\nu_{O-H\cdots O}$ (800-558 cm^{-1}) from the free ligands, indicating significant changes. The stretching band of C=O appears at 1628 cm^{-1}, with substantial absorption in the range of 3000-3500 cm^{-1}, suggesting water coordination at the ninth ligand position of Eu^{3+}. Additionally, there is a new absorption peak at 580 cm^{-1} in the synthesized material's spectrum, attributed to the stretching vibration of the Eu ← O coordinate bond. These results indicate the existence of strong interaction between the free ligands and Eu^{3+}, forming stable chelate rings.

The synthesized complexes were characterized by IR spectroscopy to confirm the presence of functional groups in the complexes. The IR spectra of Phen, HTTA and $Eu(TTA)_3Phen$, $Eu_{0.5}Tb_{0.5}(TTA)_3Phen$, $Eu_{0.5}Nd_{0.5}(TTA)_3Phen$ and $Eu_{0.5}Pr_{0.5}(TTA)_3Phen$ are shown in Fig. 6. The bands with peaks at 1587; 853 and 739 cm^{-1} are assigned to the C=N and C–H deformation vibrations of Phen, respectively. This indicates that the chemical bonds are formed between the rare earth ion and the nitrogen atom in the 1,10-phenanthroline chain. Moreover, the IR spectrum of HTTA shows a weak band at 3118 cm^{-1}, which can be assigned to the mC–H of the thiophene ring. This band is observed at frequencies (c: 3089 cm^{-1}; d: 3089 cm^{-1}) in all the complexes. Furthermore, the

typical asymmetric mC=O (HTTA) group vibrations are found at around 1662 and 1643 cm^{-1}, and shifted to 1627 and 1598 cm^{-1} upon complexation, indicating the bond formation between rare earth ions and the oxygen atom in the carbonyl group, thus confirming the formation of the complexes. In addition, the spectrum of $Eu(TTA)_3Phen$ shows no significant absorption bands in the range of 3000-3500 cm^{-1}, suggesting that water is not coordinated to the ninth coordination site of Eu^{3+} and the coordinated ligands protect the metal ion from water in the crystal structure. This result is in good agreement with previously published works [15].

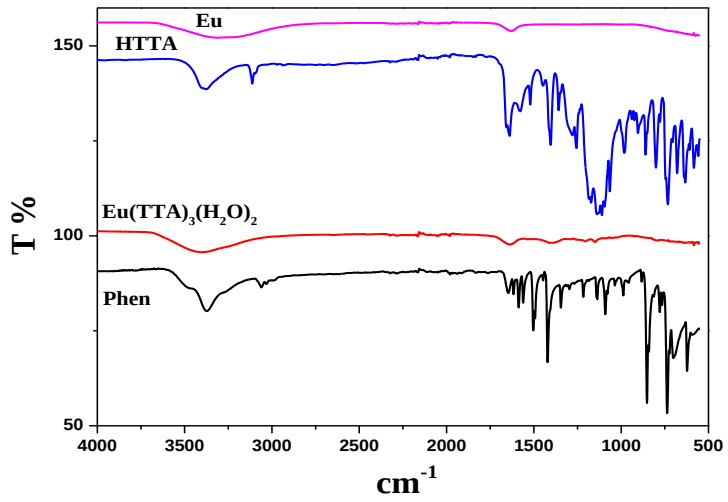

Fig. 5 . IR spectra of Eu, Phen, $Eu(TTA)_3(H_2O)_2$ and HTTA samples.

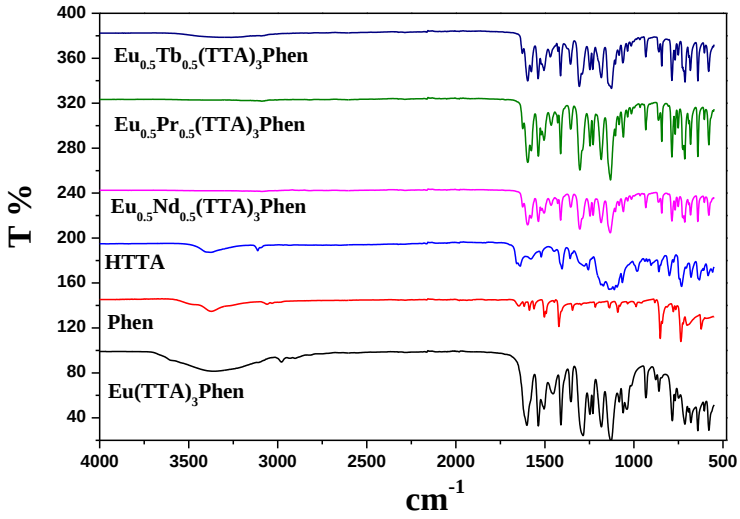

Fig. 6. IR spectra of HTTA, Phen, $Eu(TTA)_3Phen$, $Eu_{0.5}Tb_{0.5}(TTA)_3Phen$, $Eu_{0.5}Nd_{0.5}(TTA)_3Phen$, and $Eu_{0.5}Pr_{0.5}(TTA)_3Phen$ samples.

It is worth noting that similar results were also obtained for Eu^{3+}, Eu^{3+}/Tb^{3+}, Eu^{3+}/Nd^{3+} and Eu^{3+}/Pr^{3+} complexes. The band around 1591 cm^{-1} corresponds to the stretching vibration of - N=C (1,10-Phen), while the band around 740 cm^{-1} is assigned to the rC-H vibration of 1, 10-Phen. Furthermore, the typical asymmetric stretching vibration of the vC=O (TTA) group is found at around 1601 and 1539 cm^{-1}. The IR spectra of the synthesized complexes are similar to those of the pure HTTA and Phen ligands. This result is in good agreement with previously published works [7]. Thus, this confirms the successful synthesis of the $Eu_xTb_{1-x}(TTA)_3Phen$, $Eu_xNd_{1-x(}TTA)_3Phen$ and $Eu_xPr_{1-x(}TTA)_3Phen$ complexes.

The EDX spectrum was utilized in conjunction with Scanning Electron Microscopy (SEM). We conducted EDX spectral measurements of the synthesized complexes to determine the elemental composition, obtain quantitative information about the elements in the sample, and gather information on the spatial distribution of the elements within the sample. The SEM images of the $Eu_{0.5}Tb_{0.5}(TTA)_3Phen$ complex are shown in Fig. 7. The results in Fig. 7 show the presence of the elements C, O, F, S, Eu, Tb, which are consistent with the chemical composition of the compound $Eu_{0.5}Tb_{0.5}(TTA)_3(Phen)$, and the ratio of Eu^{3+}/Tb^{3+} is approximately 1:1. Based on the above results, we can conclude that we have successfully synthesized the $Eu_{0.5}Tb_{0.5}(TTA)_3(Phen)$ complex.

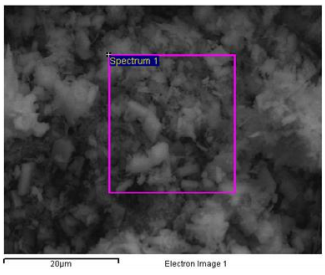

(a)

Element	Weight%	Atomic%
C K	47.07	62.61
O K	13.10	13.08
F K	24.03	20.21
S K	6.25	3.11
Eu L	4.60	0.48
Tb L	4.96	0.50
Totals	100.00	

(b)

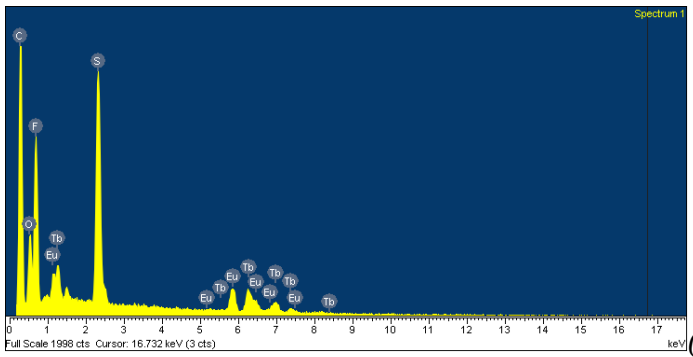

(c)

Fig. 7. (a) FESEM image; (b) Elemental composition; (c) EDX spectrum of $Eu_{0,5}Tb_{0,5}(TTA)_3(phen)$ sample.

The SEM images of the $Eu_{0.5}Nd_{0.5}(TTA)_3Phen$ complex are shown in Fig. 8. The results in Fig. 8 show the presence of the elements C, O, F, S, Eu, Nd, which are consistent with the chemical composition of the compound $Eu_{0.5}Tb_{0.5}(TTA)_3(Phen)$, and the ratio of Eu^{3+}/Pr^{3+} is approximately 1:1. Based on the above results, we can conclude that we have successfully synthesized the $Eu_{0.5}Nd_{0.5}(TTA)_3(Phen)$ complex.

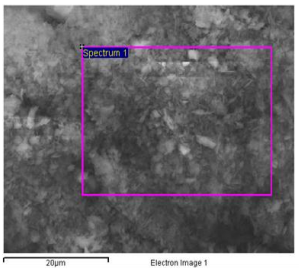

(a)

Element	Weight%	Atomic%
C K	46.15	62.81
O K	12.58	12.85
F K	22.71	19.54
S K	6.90	3.52
Nd L	5.82	0.66
Eu L	5.86	0.63
Totals	100.00	

(b)

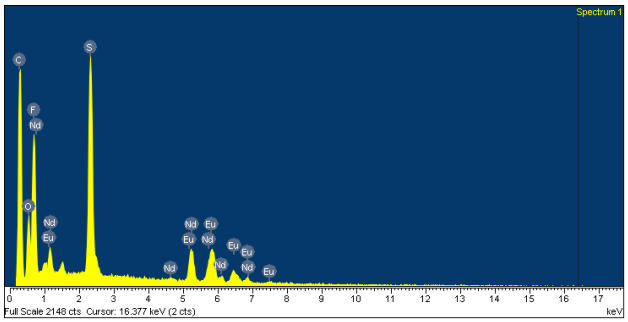

(c)

Fig. 8. (a) FESEM image; (b) Elemental composition; (c) EDX spectrum of $Eu_{0,5}Nd_{0,5}(TTA)_3(phen)$ sample.

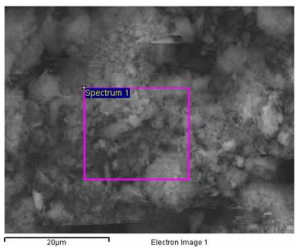

(a)

Element	Weight%	Atomic%
C K	45.44	63.54
O K	11.77	12.36
F K	20.42	18.05
S K	8.51	4.46
Pr L	6.73	0.80
Eu L	7.12	0.79
Totals	100.00	

(b)

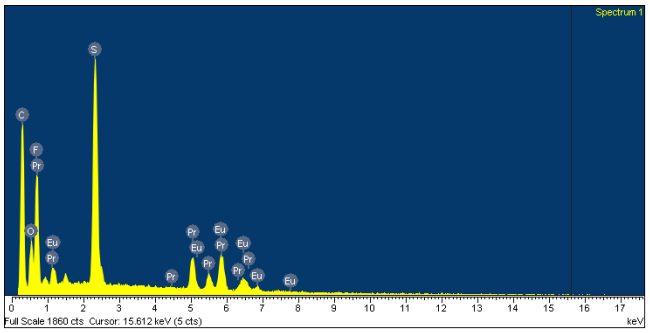

(c)

Fig. 9. (a) FESEM image; (b) Elemental composition; (c) EDX spectrum of $Eu_{0,5}Pr_{0,5}(TTA)_3(phen)$ sample.

The SEM images of the $Eu_{0.5}Pr_{0.5}(TTA)_3Phen$ complex are shown in Fig. 9. The results in Fig. 9 show the presence of the elements C, O, F, S, Eu, Pr, which are consistent with the chemical composition of the compound $Eu_{0.5}Tb_{0.5}(TTA)_3(Phen)$, and the ratio of Eu^{3+}/Pr^{3+} is approximately 1:1. Based on the above results, we can conclude that we have successfully synthesized the $Eu_{0.5}Pr_{0.5}(TTA)_3(Phen)$ complex.

3.2. Study on the luminescent properties of Lanthanides complexes

The UV-Vis spectra of HTTA, Phen, $Eu(TTA)_3Phen$, and $Eu(TTA)_3(H_2O)_2$ are shown in Fig. 10. As shown in Fig. 10, the HTTA compound has absorption peaks at wavelengths of 267 nm and 296 nm corresponding to the π - π* transition between the keto form and the enol form, respectively. The Phen compound gives absorption peaks at wavelengths of 232 nm and 264 nm corresponding to the π - π * and n - π * transition bands. Similarly, the $Eu(TTA)_3Phen$ complex has absorption wavelengths of 232, 273, and 341 nm, while the $Eu(TTA)_3(H_2O)_2$ complex has absorption wavelengths of 214, 273, and 346 nm. The spectra of the two synthesized complexes both exhibit a slight bathochromic shift of the absorption maximum, indicating the interaction between the ligand and the lanthanide.

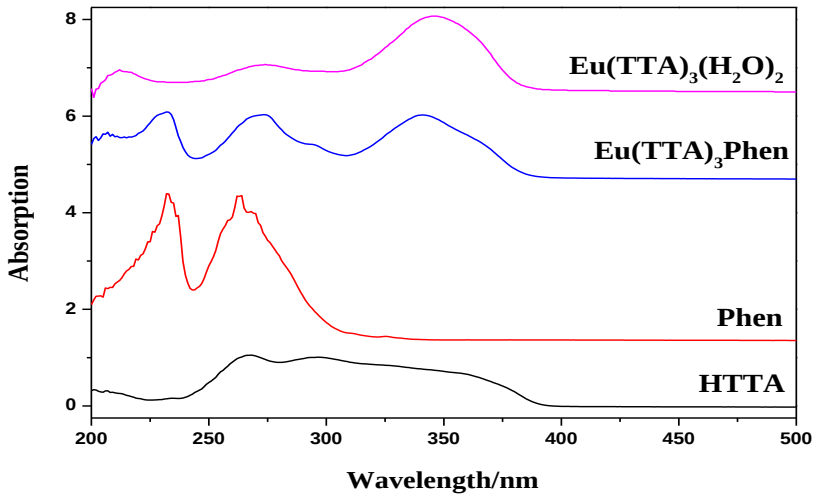

Fig. 10. UV-Vis spectrum of the complex $Eu(TTA)_3Phen$, $Eu(TTA)_3(H_2O)_2$.

The luminescence properties of the $Eu(TTA)_3Phen$ and $Eu(TTA)_3(H_2O)_2$ complex were investigated using the photoluminescence (PL) spectrum of the complex in ACN solvent. The measured results are shown in Fig. 11. For all the complexes we synthesized, the excitation spectra were measured by monitoring the fluorescence of the Eu^{3+} complex at a wavelength of 612 nm. The emission spectra of the complexes were obtained by exciting the complexes with ultraviolet light at a wavelength of 385 nm. Figure 11 shows emission spectra of the $Eu(TTA)_3Phen$ and $Eu(TTA)_3(H_2O)_2$ complex.

According to the above results, it can be seen that the 5 typical emission peaks of the $Eu(TTA)_3Phen$ complex appear at wavelengths of 580, 592, 612, 652, and 702 nm, respectively, corresponding to the transitions $^5D_0 \rightarrow {}^7F_0$, $^5D_0 \rightarrow {}^7F_1$, $^5D_0 \rightarrow {}^7F_2$, $^5D_0 \rightarrow {}^7F_3$ và $^5D_0 \rightarrow {}^7F_4$ ($\Delta J = 0, 1, 2, 3, 4$). The experimental results show that the $Eu(TTA)_3Phen$ complex in the emission spectrum at a wavelength of 612 nm corresponding to the transition $^5D_0 \rightarrow {}^7F_2$ has a stronger intensity than other fluorescence emissions, indicating that the highly polarizing chemical environment around the Eu^{3+} ion is the cause of the bright red emission of these samples. This result is fully consistent with the previously published work [7].

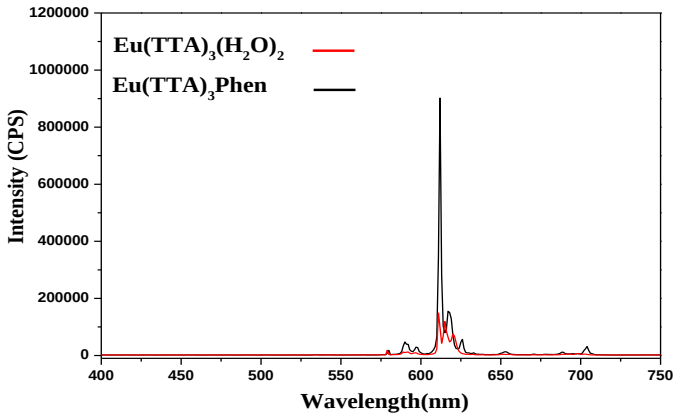

Fig. 11. Emission spectrum of the complex $Eu(TTA)_3Phen$, $Eu(TTA)_3(H_2O)_2$.

To determine the maximum absorption wavelengths, we utilized the UV-Vis spectroscopy method. The UV-Vis spectra of $Eu(TTA)_3Phen$, $Eu_{0.5}Tb_{0.5}(TTA)_3Phen$, $Eu_{0.5}Nd_{0.5}(TTA)_3Phen$, and $Eu_{0.5}Pr_{0.5}(TTA)_3Phen$ are depicted in Fig. 12. It can be observed that the absorption ranges of the synthesized complexes exhibit no significant difference compared to the corresponding pure complexes, except for a slight redshift in the absorption peaks. They all exhibit main absorption peaks in the ultraviolet region around 200 - 400 nm, with maximum absorption peaks at 231, 274, and 340 nm. This indicates that the energy absorption of these complexes primarily originates from the ligands.

Next, we conducted a study on the fluorescence capabilities of mixed complexes Eu^{3+}/Tb^{3+}, Eu^{3+}/Nd^{3+}, and Eu^{3+}/Pr^{3+} (at equal metal ratios) with TTA and Phen ligands. To compare the fluorescence abilities of these complexes, we measured the photoluminescence (PL) spectra of $Eu(TTA)_3Phen$, $Eu_{0.5}Tb_{0.5}(TTA)_3Phen$, $Eu_{0.5}Nd_{0.5}(TTA)_3Phen$, and $Eu_{0.5}Pr_{0.5}(TTA)_3Phen$ directly on the synthesized solid samples. The results are shown in Fig. 12.

Figure 12 displays emission peaks at 579, 590, 612, 651, and 703 nm, corresponding to the transitions $^5D_0 \rightarrow {}^7F_0$, $^5D_0 \rightarrow {}^7F_1$, $^5D_0 \rightarrow {}^7F_2$, $^5D_0 \rightarrow {}^7F_3$, and $^5D_0 \rightarrow {}^7F_4$ (ΔJ = 0,1,2,3,4) of the Eu^{3+} complex. Additionally, peaks at 597 nm correspond to the transition $^5D_4 \rightarrow {}^7F_4$, while peaks at 618 nm and 625 nm correspond to the transition $^5D_4 \rightarrow {}^7F_3$ of the Tb^{3+} complex.

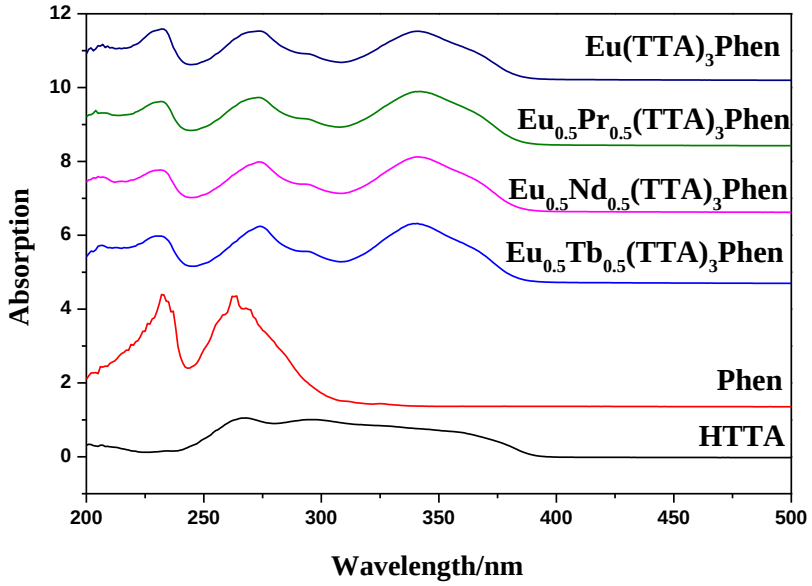

Fig. 12. UV-Vis spectrum of the complex $Eu(TTA)_3Phen$, $Eu_{0.5}Tb_{0.5}(TTA)_3Phen$, $Eu_{0.5}Nd_{0.5}(TTA)_3Phen$, and $Eu_{0.5}Pr_{0.5}(TTA)_3Phen$.

Comparing the emission intensities of the complexes at the characteristic wavelength of 612 nm, we observe that the emission intensity of $Eu_{0.5}Nd_{0.5}(TTA)_3Phen$ and $Eu_{0.5}Pr_{0.5}(TTA)_3Phen$ is the weakest. Following this, the emission intensity increases in the order of $Eu_{0.5}Tb_{0.5}(TTA)_3Phen$ and the strongest emission intensity is observed in $Eu(TTA)_3Phen$ complex.

To compare the fluorescence capabilities of the complexes, we measured the photoluminescence (PL) spectra of the $Eu_xTb_{1-x}(TTA)_3Phen$ complexes directly on the synthesized solid samples. The results are shown in Fig. 13.

Figure 13 displays emission peaks at 579, 590, 612, 651, and 703 nm, corresponding to the transitions $^5D_0 \rightarrow {}^7F_0$, $^5D_0 \rightarrow {}^7F_1$, $^5D_0 \rightarrow {}^7F_2$, $^5D_0 \rightarrow {}^7F_3$, and $^5D_0 \rightarrow {}^7F_4$ (ΔJ = 0, 1, 2, 3, 4) of the Eu^{3+} complex. Additionally, peaks at 597 nm correspond to the transition $^5D_4 \rightarrow {}^7F_4$, while peaks at 618 nm and 625 nm correspond to the transition $^5D_4 \rightarrow {}^7F_3$ of the Tb^{3+} complex.

Regarding the emission intensity of the complexes, after comparing the emission intensities at the characteristic wavelength of 612 nm, we observe that the emission

intensity of $Tb(TTA)_3Phen$ complex is the weakest. It can be observed that $Eu_{0.1}Tb_{0.9}(TTA)_3Phen$ has a ratio of Eu to Tb that is nine times smaller, yet it still ensures the luminescence intensity of the synthesized complex. Following this, the emission intensity increases in the order of $Eu_{0.9}Tb_{0.1}(TTA)_3Phen$, $Eu_{0.1}Tb_{0.9}(TTA)_3Phen$, and the complex with the strongest emission intensity is $Eu_{0.5}Tb_{0.5}(TTA)_3Phen$. Therefore, we can conclude that for the $Eu_xTb_{1-x}(TTA)_3Phen$ complex to achieve the best fluorescence result, the optimal ratio to use is 5:5 (x = 0.5).

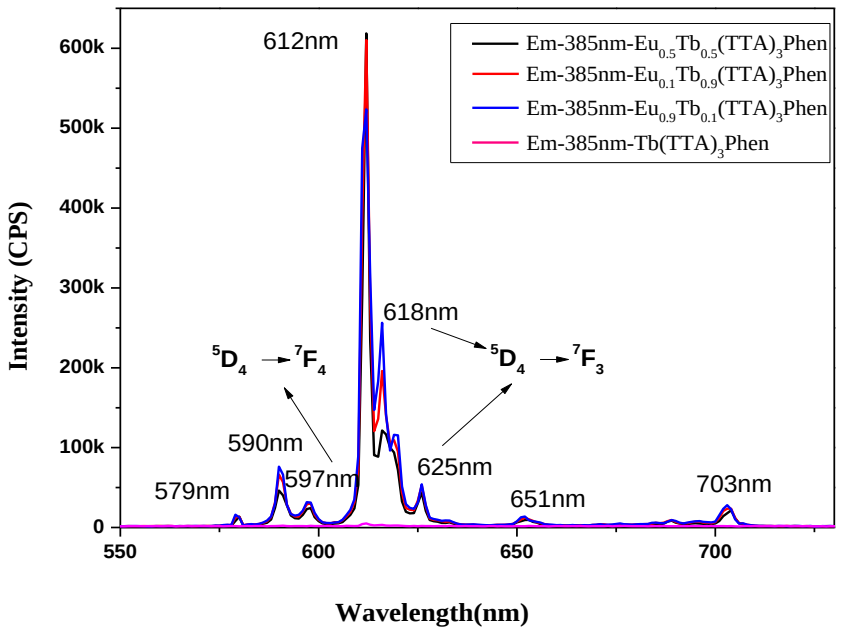

Fig. 13. Emission spectrum of the complex $Eu_xTb_{1-x}(TTA)_3Phen$.

The combination of europium with other metals such as Tb, Nd, Pr, along with ligands to form lanthanide complexes marks a new advancement in the research field of the fluorescence of these complexes. It not only represents an effort to expand our understanding of the optical properties of lanthanide complexes but also signifies a unique integration of various elements, offering vast potential applications across multiple domains, especially in the military sector. The amalgamation of different metals not only contributes to diversifying input sources but also ensures continuity and stability in chemical production processes. This aspect is particularly crucial in the military industry, where stability and continuity are key to ensuring efficiency and safety. These novel lanthanide complexes not only present new opportunities in scientific research but also hold significant potential in enhancing detection capabilities and countering threats posed by various types of chemical warfare agents.

4. Conclusion

The synthesis of Lanthanide complexes was successfully studied, using IR, UV-Vis, EDX spectra to prove the structure, and analyzed the PL spectra to compare the luminescence properties of the complexes. The results indicate that the structure Eu_xM_{1-x}(TTA)Phen (M: Tb, Nd, Pr; x = 0.1; 0.5; 0.9; 1.0) gives stronger luminescence. Along with that, combining with metals other than Eu has contributed to mastering raw material sources and diversifying material solutions to meet production needs in the armed forces. With continued research and development, Lanthanide-based sensors could help our military counter the threats from chemical warfare.

Acknowledgement

This research is funded by Le Quy Don Technical University Research Fund under the grant number 2024.ĐH.06.

References

[1] J. Geoghegan and J. L. Tong, "Chemical warfare agents", *Continuing Education in Anaesthesia Critical Care & Pain*, Vol. 6, Iss. 6, 2006, pp. 230-234. DOI: 10.1093/bjaceaccp/mkl052

[2] V. Kumar, "Chromo-fluorogenic sensors for chemical warfare agents in real-time analysis: Journey towards accurate detection and differentiation", *Chemical Communications*, Vol. 57, pp. 3430-3444, 2021. DOI: 10.1039/d1cc00132a

[3] F. R. Sidell, J. Newmark, and J. H. McDonough, "Chapter 5: Nerve Agents", *Medical Aspects of Chemical Warfare*, 2013, pp. 155-219. DOI: 10.1002/0471238961.0308051308011818.a01.pub3

[4] W. Meng, A. C. Sedgwick, N. Kwon *et al.*, "Fluorescent probes for the detection of chemical warfare agents", *Chemical Society Reviews*, Vol. 52, pp. 601-662, 2023. DOI: 10.1039/d2cs00650b

[5] H. Zhang and D. M. Rudkevich, "A FRET approach to phosgene detection", *Chemical Communications*, Vol. 12, pp. 1238-1239, 2007. DOI: 10.1039/B614725A

[6] Y. Hu, L. Chen, H. Jung *et al.*, "Effective strategy for colorimetric and fluorescence sensing of phosgene based on small organic dyes and nanofiber platforms", *ACS Applied Materials & Interfaces*, Vol. 8, pp. 22246-22252, 2016. DOI: 10.1021/acsami.6b07138

[7] L. Yuguang, Z. Jingchang, C. Weiliang, Z. Fujun, and X. Zheng, "Syntheses and Characterization of Binuclear Complexes $Tb_{1-x}Eu_x(TTA)_3$Phen", *Journal of Rare Earths*, Vol. 25, pp. 296-301, 2007. DOI: 10.1016/S1002-0721(07)60425-6

[8] B. Zhu, R. Sheng, T. Chen *et al.*, "Molecular engineered optical probes for chemical warfare agents and their mimics: Advances, challenges and perspectives", *Coordination Chemistry Reviews*, Vol. 463, 2022. DOI: 10.1016/j.ccr.2022.214527

[9] V. Kumar and E. V. Anslyn, "A selective and sensitive chromogenic and fluorogenic detection of a sulfur mustard simulant", *Chemical Science*, Vol. 4, pp. 4292-4297, 2013. DOI: 10.1039/C3SC52259h

[10] M. Seshadri, V. de C. dos Anjos, and M. J. V. Bell, "Luminescent glass for lasers and solar concentrators", *Luminescence - An Outlook on the Phenomena and their Applications*, InTech, p. 28, 2016. DOI: 10.5772/65057

[11] F. Ramos-Lara, A. Lira C., M. O. Ramírez *et al.*, "Optical spectroscopy of Nd^{3+} ions in poly(acrylic acid)", *Journal of Physics: Condensed Matter*, Vol. 18, Iss. 34, pp. 7951-7959, 2006. DOI: 10.1088/0953-8984/18/34/008

[12] S. Mitra and S. Jana, "Intense orange emission in Pr^{3+} doped lead phosphate glass", *Journal of Physical and Chemistry of Solids*, Vol. 85, pp. 245-253, 2015. DOI: 10.1016/j.jpcs.2015.05.007

[13] G. H. Dennison and M. R. Johnston, "Mechanistic insights into the luminescent sensing of organophosphorus chemical warfare agents and simulants using trivalent lanthanide complexes", *Chemistry - A European Journal*, Vol. 21, pp. 1-12, 2015. DOI: 10.1002/chem.201406213

[14] P. Lu, Y. Wang, L. Huang *et al.*, "Tb^{3+}/Eu^{3+} complex-doped rigid nanoparticles in transparent nanofibrous membranes exhibit high quantum yield fluorescence ", *Nanomaterials*, Vol. 10, 2020. DOI: 10.3390/nano10040694

[15] E. R. Menzel, L. W. Menzel, and J. R. Schwierking, "A photoluminescence-based field method for detection of traces of explosives", *The Scientific World Journal*, Vol. 4, pp. 948-955, 2004. DOI: 10.1100/tsw.2004.126

NGHIÊN CỨU ẢNH HƯỞNG CỦA CÁC ION KIM LOẠI NHÓM LANTHANIDE ĐẾN HIỆU ỨNG HUỲNH QUANG CỦA PHỨC CHẤT $EU(TTA)_3(H_2O)_2$ VÀ $EU(TTA)_3PHEN$

Vũ Ngọc Doãn[1], Đỗ Quang Tuấn[1], Lê Minh Đông[1], Cao Hải Thường[1]

[1]*Khoa Hóa - Lý kỹ thuật, Trường Đại học Kỹ thuật Lê Quý Đôn*

Tóm tắt: Trong nghiên cứu này, các tác giả đánh giá hiệu ứng phát huỳnh quang của phức $Eu(TTA)_3(H_2O)_2$ và $Eu(TTA)_3$(Phen) khi có mặt nhiều ion kim loại họ lanthanide khác. Đặc tính huỳnh quang của các phức hợp này được nghiên cứu để tìm hiểu khả năng tương tác của chúng với các ion lanthanide khác và ảnh hưởng của chúng đến sự phát xạ huỳnh quang của hệ phức chất. Phương pháp phân tích quang phổ được sử dụng để kiểm tra sự ảnh hưởng của các ion lanthanide khác nhau đến sự phát huỳnh quang của phức $Eu(TTA)_3(H_2O)_2$ và $Eu(TTA)_3$(Phen). Đặc điểm cấu trúc sản phẩm được xác định bằng phương pháp quang phổ IR, UV-Vis và EDX. Tính chất quang của phức chất được nghiên cứu bằng phương pháp quang phổ huỳnh quang. Kết quả cho thấy cấu trúc $Eu_xM_{1-x}(TTA)_3$Phen (M: Tb, Nd, Pr; x = 0,1; 0,5; 0,9; 1,0) cho khả năng phát quang mạnh hơn ở bước sóng λ_{ex} = 385 nm.

Từ khóa: *Lanthanide; phản ứng đa thành phần; huỳnh quang.*

Received: 06/04/2024; Revised: 18/09/2024; Accepted for publication: 30/10/2024

❑